PCCP

Accepted Manuscript

ROYAL SOCIETY OF CHEMISTRY

www.rsc.org/pccp

Spectroscopic Characterization of $C_7H_3^+$ and $C_7H_3^\bullet$: Electronic Absorption and Fluorescence in 6 K Neon Matrices

Arghya Chakraborty, Jan Fulara, Rainer Dietsche, John P. Maier*

Department of Chemistry, University of Basel, Klingelbergstarasse 80, CH-4056, Basel, Switzerland

Abstract

Mass selective deposition of $C_7H_3^+$ (*m/z*=87) into solid neon reveals the **1** $^1A_1 \leftarrow$ **X** $^1A_1$ electronic absorption system of hepta-1,2,3,4,5,6-heptahexaenylium cation **B**$^+$ $[H_2CCCCCCCH]^+$ with origin band at 441.3 nm, **1** $^1A' \leftarrow$ X $^1A'$ transition of 2,4-pentadiynylium,1-ethynyl cation **C**$^+$ $[HCCCHCCCCH]^+$ starting at 414.6 nm and the **1** $^1A_1 \leftarrow$ X $^1A_1$ one of cyclopropenylium,1,3-butadiynyl cation **A**$^+$ $[HCCCCC<(CH=CH)]^+$ with onset 322.2 nm. Vibrationally resolved fluorescence was observed for isomer **B**$^+$ upon laser excitation of the absorption bands in the **1** $^1A_1 \leftarrow$ **X** $^1A_1$ transition. After neutralization of the cations in the matrix five absorption systems of the C_7H_3 neutral radicals starting at 530.3, 479.4, 482.3, 325.0 and 302.5 nm were detected. These were identified as the **1** $^2A' \leftarrow$ **X** $^2A'$ and **2** $^2A' \leftarrow$ **X** $^2A'$ electronic transitions of 2-(buta-1,3-diynyl)cycloprop-2yl-1-1ylidene **E**$^\bullet$ $[HCCCCC<(C=CH_2)]^\bullet$, **1** $^2B_1 \leftarrow$ **X** $^2B_1$ of 1,2,3,4,5,6-heptahexaenyl **B**$^\bullet$ $[H_2CCCCCCCH]^\bullet$, **3** $^2B_1 \leftarrow$ **X** $^2B_1$ of 3-buta-1,3-diynyl-cyclopropenyl **A**$^\bullet$ $[HCCCCC<(CH=CH)]^\bullet$ and **2** $^2B_1 \leftarrow$ X $^2A_2$ transition of 1,2-divinylidene-cyclopropanyl radical **F**$^\bullet$ [HCC-cyc-(CCHC)-CCH]$^\bullet$, respectively. The assignment is based on calculated vertical excitation energies using the CASPT2 method. Comparison of the calculated harmonic vibrational frequencies with those inferred from the spectra support the assignment.

1. Introduction

A variety of unsaturated species including polycyclic aromatic systems are produced during combustion of hydrocarbons in an oxygen deficient environment, as has been established by gas chromatography and molecular beam mass spectrometry (MBMS).[1-5] The production of larger aromatic systems in soot starting from small hydrocarbons is not entirely understood. Theoretical kinetics and MBMS suggest that $C_{2n+1}H_3$ systems have a vital role.[5-9] The recombination mechanism of propargyl radical, $C_3H_3^{\bullet}$, is considered as one of the key processes for larger aromatics formation.[10-12] Thus the $C_{2n+1}H_3^{\bullet}$ class of molecules presents an intriguing subject for a spectroscopic exploration and the identification of the electronic absorptions of the various isomers will enable their in situ monitoring in soot formation.

The propargyl radical has been studied by microwave,[13] infrared,[14,15] photoelectron[16] and electronic[17,18] spectroscopies. Propargyl cation also has been characterized by electronic and infrared spectroscopy.[19,20] The next member of this series, the $C_5H_3^{\bullet}$ radical, has been proposed as a reactive intermediate during the photodissociation of benzene.[21] It can be formed in fuel rich flames and play a role in polycyclic aromatic hydrocarbon formation.[8,21,22] In fact, the *m/z*=63 peak $C_5H_3^+$ is often found in the mass spectra of hydrocarbons. There is only circumstantial experimental and computational understanding on $C_7H_3^+$ and $C_7H_3^{\bullet}$ isomers except for one electronic spectrum recorded in the gas phase by a resonant two-color-two-photon-ionization (R2C2PI) technique.[23]

Interstellar clouds contain a rich collection of exotic molecular systems because of very low density and temperature. In the laboratory, unstable organic systems like carbon chains, combined with cyclic rings and with heteroatoms have been studied by microwave spectroscopy.[24,25,26] The $C_7H_3^+$ and $C_7H_3^{\bullet}$ species may also be relevant in the planetary atmosphere of Titan.[27]

The present study focuses on the characterization of $C_7H_3^+$ and $C_7H_3^{\bullet}$ species isolated in neon matrices at 6 K by electronic spectroscopy. $C_7H_3^+$ or $C_7H_3^-$ are produced in ion sources, then mass selected and subsequently neutralized. On the basis of the electronic excitation energies obtained by CASPT2 calculations after ground state optimization of the possible isomers, the assignments of the observed absorptions have been made.

2. Experimental

The approach used combines mass spectrometry with matrix isolation technique.[28] Ions are generated in a hot-cathode discharge source from diverse organic vapors and extracted through electrostatic lenses. The ion beam is then led into a quadrupole filter for mass selection. Subsequently, the ions are co-deposited with excess of neon, including traces (1:20000) of chloromethane (CH_3Cl), on a rhodium coated sapphire substrate held at 6 K. CH_3Cl is added to diminish the space charge during growth of matrix and to suppress neutralization of the cations. It captures electrons released from metal surface near the matrix by the impinging of cations with ~50 eV energy. The Cl^- anions, formed by dissociative electron attachment to CH_3Cl, balance the charge.[30,31] The matrix is grown to 100-150 μm thickness.

The spectra are recorded in the 200−1100 nm range in a "wave-guide" manner.[29] The detection system consists of a 0.3 m spectrograph equipped with three rotatable gratings and two wavelength specific CCD cameras. Light after passing through the 20 mm length of the matrix, parallel to the substrate surface, is collected by a lens onto a bundle of quartz fibers and into the spectrograph, wavelength dispersed, and recorded by a CCD camera. Halogen and a high pressure xenon arc lamp are the two light sources used.

The species trapped in neon were excited at an incident angle ~45° to the cold substrate surface with a pulsed, tunable laser of bandwidth ~3 cm^{-1} and energy 2-30 mJ. The

emission was collected perpendicular to the matrix surface and 45° to the laser beam. The light collected by the optical fibers was transferred to the spectrograph, dispersed, and recorded by a CCD camera, as for the absorption measurements. The measurements were started at ~2 nm longer wavelength than the excitation one to avoid saturation of the camera by the scattered laser light.

The cations and anions with *m/z*=87 were produced using different ion sources.[28] Toluene was used as a precursor of $C_7H_3^-$, while $C_7H_3^+$ was generated from a 1:1 mixture of diacetylene and propyne. Indene is a rich source for $C_7H_n^+$ ions and m/z=89, $C_7H_5^+$, is the strongest peak after the parent ion in the mass spectrum of C_9H_8.

3. Results and Discussion

3.1 Absorption

Strong absorptions are found in the 300−450 nm range (Figure 1) along with some weaker ones between 470 and 540 nm after deposition of mass selected $C_7H_3^+$ in a neon matrix containing CH_3Cl. The strongest narrow band is seen at 441.3 nm, and that of a broader peak at 414.6 nm (Figure 1, black trace). In addition, a system with onset at 322.2 nm is apparent. To distinguish absorptions of the cations from neutrals the matrix was exposed to $\lambda > 260$ nm photons from a medium pressure mercury lamp. The Cl^- anions generated from CH_3Cl release electrons which recombine with $C_7H_3^+$ producing neutral species. The intensity of the absorption systems commencing at 441.3, 414.6 and 322.2 nm decreased whereas the 325 nm bands and weaker ones around 530.3, 482.3 nm gained in intensity after irradiation (green traces, Figure 1). A moderately intense band with doublet structure is present in the spectrum around 305 nm. One component of this decreases and other increases upon irradiation due to the superposition of a cationic and neutral absorption. The absorptions which diminish are attributed to $C_7H_3^+$ while one which gain in intensity to the corresponding neutrals. The two weak bands at 448 and 407 nm (Figure 1, black trace) that diminish after

irradiation are due to *l*-HC_7H^+, a polyacetylene cation,[30] formed by collisionally-induced fragmentation of $C_7H_3^+$ during growth of the matrix.

To distinguish absorptions of the primary isomers from the collision-induced ones, $C_7H_3^+$ ions with 90 eV kinetic energy were deposited. The spectrum obtained (blue trace, Figure 1) is compared with the one recorded with 50 eV kinetic energy. The spectra were normalized to the intensity of the strongest band of $C_7H_3^+$ at 441.3 nm. As expected the absorptions of the fragment ions, l-HC_7H^+, are much stronger with 90 eV deposition energy. The bands of neutral species, which gained intensity upon UV irradiation, are stronger in this spectrum. Additionally, a moderately intense system at 505 nm appeared. It is identical with the electronic spectrum of l-$HC_7H^\bullet$ obtained previously[31] as shown in the light blue trace of Figure 1.

Figure 2 is a close up of the region where the differences in the spectra recorded with kinetic energies of 50 and 90 eV are pronounced. Apart from the absorptions of l-HC_7H^+, two systems of neutral C_7H_3 with onsets at 530.3 and 482.3 nm are apparent. The intensity of these absorptions are much stronger in the spectrum obtained by mass selected deposition of $C_7H_3^-$ anions followed by irradiation (pink trace, Figure 2). The relative intensities of the 530.3 and 482.3 nm systems vary with deposition energy and also upon irradiation, which suggests that the systems belong to two $C_7H_3^\bullet$ isomers. The origin of the 530.3 nm system lies close to the onset of the 2-(buta-1,3-diynyl)cycloprop-2yl-1-1ylidene radical (isomer $\mathbf{E}^\bullet$ in Chart 1) absorption, identified at 528.3 nm in the gas-phase[23] and the pattern of the vibrational progression is similar.

The enhancement of isomer $\mathbf{E}^\bullet$ absorption with higher kinetic energy deposition, as well as in $C_7H_3^-$ anion deposition at even higher kinetic energy ~150 eV, reveals that $\mathbf{E}^\bullet$ is produced as a secondary product during matrix growth. The primary ions should have a similar structure as $\mathbf{E}^\bullet$ - a cyclic three-membered carbon ring with a butynyl group C_4H attached. The $\mathbf{E}^\bullet$ isomer and the corresponding primary cation differ only in the position of

hydrogen atoms. Stronger absorption of l-HC_7H^+ seen in the spectra obtained with higher than 50 eV deposition energy suggests that the other primary $C_7H_3^+$ cations have an open chain structure, for which the removal of a hydrogen atom is facile and leads to the enhancement of the l-HC_7H^+ absorptions. Though the identification of the secondary products of $C_7H_3^+$ produced under higher kinetic energy conditions provide a hint about the structure of the primary cations, the information derived from the spectra is not sufficient to assign the observed absorptions to specific species. Theoretical studies on the stability of different isomers of $C_7H_3^+$ and the corresponding neutrals as well as excitation energies of these species are needed and have been carried out (*vide infra*).

3.2 Fluorescence

All the intense absorption bands seen in Figure 1 were excited with a laser for fluorescence detection after depositing $C_7H_3^+$ with neon. The concentration of the CH_3Cl scavenger was kept lower (1: 50000) to have enough cations as well as neutrals in the matrix. The neutral systems at 530.3 and 482.3 nm do not fluoresce. However, a structured emission was detected, commencing at 442.7 nm and extending to 514 nm, after laser excitation of the sharp band at 441.3 nm (Figure 3). The same fluorescence spectrum, though less intense, was obtained when the laser photons matched the wavelengths of weak absorption peaks lying 558, 809 and 1087 cm^{-1} above the 441.3 nm origin. This confirms that these absorption bands belong to the same electronic system. Origin of the fluorescence and absorption overlap at 442.4 nm which is the zero-phonon line (ZPL) of the two spectra. The wavelengths of the fluorescence bands are collected in Table 2. No fluorescence was detected upon excitation of the 414.6 nm and 322.2 nm systems of $C_7H_3^+$ and 325 and 303 nm of neutrals.

3.3 Computations: comparison with experiment

Geometry optimization of plausible twelve cations and their neutral isomers (Table S1) was carried out by density functional theory (DFT) with the B3LYP functional and the cc-pVDZ basis set using the Gaussian 09 program suite.[32] Harmonic vibrational frequencies in

the ground state were calculated to check whether the structures are real minima on the potential energy surface (PES). The geometries of all species were next refined with Moller–Plesset perturbation[33] (MP2) method using the cc-pVDZ basis set and used as a starting point for excitation energies calculations.

The vertical excitation energies were calculated using a second order multiconfigurational perturbation theory (CASPT2) implemented in the Molcas program package.[34,35]. 13 electrons partitioned in 13 orbitals formed the active space and six roots were calculated for the irreducible representation of each species. The vertical excitation energies obtained are given in Table S2 and compared with the origin band positions in the spectra of $C_7H_3^+$ and $C_7H_3^\bullet$ in neon matrices. The results for the five lowest energy structures; $\mathbf{A}^+$, $\mathbf{B}^+$, $\mathbf{C}^+$, $\mathbf{F}^+$, $\mathbf{J}^+$ and for isomer $\mathbf{E}^\bullet$ for which the electronic transition starting at 530.3 nm was already identified in a gas – phase study,[23] are discussed in the next paragraphs. The structure of the **A**, **B**, **C**, **F, J** and **E** molecules is presented in Chart 1 together with the ground state energies calculated for the cationic, anionic and neutral forms. The bond lengths for the cations, calculated with the MP2 method, are shown. The global minimum on the $C_7H_3^+$ PES, predicted by both theoretical methods, is isomer $\mathbf{A}^+$, a three - membered carbon ring fused with the linear C_4H chain. The second lowest energy structure $\mathbf{F}^+$ has the same three - member carbon ring motif but with two ethynyl groups attached. The next in energy isomer $\mathbf{J}^+$ - fused three and six carbon rings – is located 40 kJ/mol above $\mathbf{A}^+$ according to MP2 calculations. Isomers $\mathbf{B}^+$ and $\mathbf{C}^+$ are almost isoenergetic and lie 61 and 69 kJ/mol above $\mathbf{A}^+$. At the DFT level $\mathbf{B}^+$ is more stable than $\mathbf{J}^+$. Cation $\mathbf{E}^+$ lies 452 kJ/mol above the most stable $\mathbf{A}^+$. However $\mathbf{E}^+$ is also focused on because the electronic transition of $\mathbf{E}^\bullet$ is observed in the present studies. The most stable structure of neutral C_7H_3 is isomer **J**. The relative stability and the energy order of the $C_7H_3^+$ isomers obtained from the previous DFT calculations[23] with the smaller basis set differs from the present results. The energies obtained from the MP2 calculations are

the more reliable. However both DFT and MP2 methods fail to describe properly the electronic systems in the case of near degeneracy. More advanced methods are needed for this purpose.

Isomers A^+, $A^\bullet$ and $F^\bullet$

The ground state of the two lowest energy $C_7H_3^+$ cations, $\mathbf{A}^+$ and $\mathbf{F}^+$, has X $^1A_1$ symmetry. The MS CASPT2 calculations predict two dipole - allowed electronic transitions to the **1** $^1A_1$ and **2** $^1A_1$ states below 6.5 eV (Table 3). The first **1** $^1A_1$ electronic state of $\mathbf{A}^+$ and $\mathbf{F}^+$ lies at 4.13 and 5.46 eV above the X $^1A_1$ state, with oscillator strengths of the transitions 0.40 and 0.13, respectively. The second **2** $^1A_1 \leftarrow$ X $^1A_1$ around 6 eV is two orders of magnitude weaker in intensity. These results are consistent with earlier CASSCF and MRCI calculations on cyclic $C_3H_3^+$ which predict a dipole allowed electronic transition around 8 eV.[19] Substitution of two hydrogen atoms in c-$C_3H_3^+$ with two ethynyl groups (isomer $\mathbf{F}^+$) shifts this transition to 5.46 eV. A much lower energy 4.13 eV was predicted for $\mathbf{A}^+$ where one hydrogen atom of c-$C_3H_3^+$ is replaced with a butynyl group, because the electrons are delocalized over a larger distance.

c-$C_3H_3^+$, produced from cyclic and acyclic precursors, has been studied in neon matrices.[19] Though its electronic transition was not observed due to the wavelength being out of the detection range of the setup, the presence of c-$C_3H_3^+$ was proven by infrared measurements.[19] One can expect that $\mathbf{A}^+$ and $\mathbf{F}^+$ are also formed in the present experiments and trapped in the neon matrix, as the conditions were similar to those for c-$C_3H_3^+$. However isomer $\mathbf{F}^+$, with electronic transition around 5.46 eV, could not be observed for technical reasons: the scattering of light from the matrix. The calculations for the neutral $\mathbf{F}^\bullet$ predict three electronic transitions from the X $^2A_2$ ground state to the **1** $^2B_1$, **2** $^2B_1$ and **3** $^2B_1$ states at

1.15, 4.44 and 5.64 eV and oscillator strengths 0.03, 0.04 and 0.19, respectively. These at 1.15 and 5.64 eV are outside the range of detection system.

Cation $\mathbf{A}^+$, contrary to $\mathbf{F}^+$, has the strong (f= 0.40) $\mathbf{1}\ ^1A_1 \leftarrow X\ ^1A_1$ transition at lower energy (4.13 eV; 300 nm), close to the 322.3 nm absorption system of $C_7H_3^+$. In this region, MS-CASPT2 calculations predict also a moderately intense (f=0.064) $\mathbf{1}\ ^1B_2 \leftarrow X\ ^1A_1$ transition for isomer J^+ (E = 4.30 eV) and a strong one $\mathbf{1}\ ^1A_1 \leftarrow X\ ^1A_1$ (f= 0.54) for isomer K^+ with energy 4.36 eV (Table S2). Because the oscillator strength of the electronic transition of isomer J^+ is an order of magnitude smaller than for the $\mathbf{1}\ ^1A_1 \leftarrow X\ ^1A_1$ transition of A^+ and isomer K^+ has an exotic structure and lies much higher in energy on the PES than A^+, we therefore assign the 322.3 nm absorption system of $C_7H_3^+$ to the $\mathbf{1}\ ^1A_1 \leftarrow X\ ^1A_1$ transition of A^+. The calculations overestimate the energy by 0.3 eV. This may be partly because the experimental data are compared with the vertical excitation energy instead with the adiabatic value.

Isomer $\mathbf{A}^+$ is likely a progenitor of neutral $\mathbf{E}^\bullet$ in the higher kinetic energy deposition experiments, because these two species have the same carbon skeleton (three membered carbon ring with C_4H attached) and differ only in the position of two hydrogen atoms. Cations $\mathbf{A}^+$, during hard landing on the matrix surface, possesses enough internal energy to rearrange the two hydrogen atoms.

The section of the electronic spectrum, where the absorptions of $\mathbf{A}^+$ are present, is shown in Figure 4. Three vibrational bands located 529, 1945 and 2464 cm^{-1} above the origin belong to this system and correspond to the excitation of the ν_9, ν_4 modes and their combinations. Harmonic vibrational frequencies in the ground state of $\mathbf{A}^+$ calculated at the MP2 level are 538 and 2098 cm^{-1}. The wavelengths of the band maxima of $\mathbf{A}^+$ and the assignment are given in Table 1.

Two absorption bands of neutral species at 325 and 303 nm are present and likely belong to two different isomers of $C_7H_3^\bullet$. The calculations predict a moderately intense

(f = 0.04) **2** $^2B_1 \leftarrow X\ ^2A_2$ transition for $\mathbf{F}^{\bullet}$ at 4.44 eV and a stronger (f = 0.13) **3** $^2B_1 \leftarrow \mathbf{X}\ ^2B_1$ one at 4.76 eV of $\mathbf{A}^{\bullet}$. Other higher energy structures of C_7H_3 are excluded from consideration because much weaker electronic transitions for these species are predicted in this region (Table S2). The 325 nm system is tentatively assigned to the **2** $^2B_1 \leftarrow X\ ^2A_2$ transition of $\mathbf{F}^{\bullet}$ and the 303 nm absorption to **3** $^2B_1 \leftarrow \mathbf{X}\ ^2B_1$ of $\mathbf{A}^{\bullet}$. The calculations overestimate the excitation energy of these transitions by ~ 0.6 eV for both isomers.

Isomers $\mathbf{B}^+$, $\mathbf{B}^{\bullet}$ and $\mathbf{C}^+$

The 390 – 460 nm section of the electronic spectrum measured after deposition of *m/z* = 87 cations (Figure 5) shows two absorption systems commencing at 441.3 nm (2.81 eV) and 414.6 nm (2.99 eV) belonging to two $C_7H_3^+$ isomers. Only four isomers, among all considered structures for which excitation energies were calculated, possess stronger electronic transitions in this region. These are $\mathbf{B}^+$, $\mathbf{C}^+$, $\mathbf{G}^+$ and $\mathbf{H}^+$. The two latter higher energy structures can be excluded because they also have even stronger transitions around 300 nm (Table S2), in conflict with observations. Isomers $\mathbf{B}^+$ and $\mathbf{C}^+$ are open chain structures (Chart 1) and are good candidates for the absorptions observed. Both cations, after removal of one hydrogen atom, can readily produce the *l*-HC_7H^+ fragment ion as observed in the higher kinetic energy studies.

The calculations predict a strong $\mathbf{1}^1A_1 \leftarrow \mathbf{X}^1A_1$ transition (f = 0.33) at 2.99 eV and a two orders of magnitude weaker one at 3.95 eV for $\mathbf{B}^+$; the first excited $\mathbf{1}^1A'$ state for $\mathbf{C}^+$ is 3.13 eV above the X $^1A'$ ground state with oscillator strength 0.64. Three other excited electronic states of $\mathbf{C}^+$ lie 4.2 – 5.2 eV above X $^1A'$, however the oscillator strengths are two orders of magnitude smaller than to the $\mathbf{1}^1A'$ state. The energy of the $\mathbf{1}^1A_1 \leftarrow \mathbf{X}^1A_1$ transition of $\mathbf{B}^+$ matches with the onset at 441.3 nm (2.81 eV) of the strongest absorption system. Also the origin of the second system at 414.6 nm (2.99 eV) correlates well with the energy of the $\mathbf{1}\ ^1A' \leftarrow X\ ^1A'$ transition of $\mathbf{C}^+$**.** Therefore, the absorptions in the spectrum shown in Figure 5 are assigned to the $\mathbf{1}^1A_1 \leftarrow \mathbf{X}^1A_1$ of $\mathbf{B}^+$ and $\mathbf{1}^1A' \leftarrow X\ ^1A'$ transitions of $\mathbf{C}^+$, respectively.

Isomer $\mathbf{B}^+$ is a protonated form of *l*-$HC_7H^{\bullet}$. In the case of triacetylene cation, addition of one hydrogen atom produces $HC_6H_2^+$, which has a similar structure as $\mathbf{B}^+$. Addition of one hydrogen atom shifts the origin band from 604.2 nm for HC_6H^+ to 378.6 nm for $HC_6H_2^+$.[36,37] Similarly the absorption of $\mathbf{B}^+$ (at 441.3 nm) is shifted ~160 nm to the blue in comparison to HC_7H^+ (599.8 nm).[30]

The vibrational bands present in the absorption and fluorescence spectra of $\mathbf{B}^+$ are assigned to specific normal modes using the MP2 calculated, harmonic vibrational frequencies in the ground state of the cation (Table 2). Four totally symmetric a_1 modes: ν_9, ν_8, ν_5 and ν_2 are active in the fluorescence spectrum of $\mathbf{B}^+$ and only the two former vibrations in the absorption. There is an absorption peak between the ν_9 and ν_8 bands, 809 cm^{-1} above the origin, which belongs to $\mathbf{B}^+$ because the fluorescence starting at ~442 nm was detected. This band arises from the excitation of two quanta of the ν_{21} (b_2) mode. In the spectrum of $\mathbf{C}^+$ two absorption peaks located 462 and 725 cm^{-1} above the origin at 414.6 nm are apparent. The first one is hidden under the l-HC_7H^+ band. They are attributed to ν_{14} and ν_{10} mode excitations by comparison with the 472 and 776 cm^{-1} calculated ground state vibrational frequencies of $\mathbf{C}^+$.

As the electronic transitions of $\mathbf{B}^+$ and $\mathbf{C}^+$ are detected one can expect that $\mathbf{B}^{\bullet}$ and $\mathbf{C}^{\bullet}$ should also be present. A good candidate for these species is the absorption system starting at 482.3 nm (2.57 eV) which gains in intensity upon UV irradiation (Figure 6). The calculations predict a weak (f = 0.002) $\mathbf{1}\ ^2B_1 \leftarrow \mathbf{X}\ ^2B_1$ transition for $\mathbf{B}^{\bullet}$ at 2.46 eV, the $\mathbf{1}\ ^2A'' \leftarrow \mathbf{X}\ ^2A''$ transition of $\mathbf{C}^{\bullet}$ at 3.21 eV with oscillator strength 0.03. Due to a better match of the calculated excitation energy of $\mathbf{B}^{\bullet}$ with the observations, 482.3 nm system is assigned to its $\mathbf{1}\ ^2B_1 \leftarrow \mathbf{X}\ ^2B_1$ transition. Table 1 lists the absorption band maxima and the assignment for the systems of $\mathbf{B}^+$, $\mathbf{B}^{\bullet}$ and $\mathbf{C}^+$.

Isomer E•

The absorption at 530.3 nm shown in Figure 6 belongs to isomer **E•** identified in the gas phase studies at 528.8 nm and assigned to the origin band of the **1** $^2A' \leftarrow$ **X** $^2A'$ transition.[23] Some unassigned bands around 481 and 474 nm were also reported. The 479.4 nm absorption system in the neon matrix behaves in a similar fashion to that of 530.3 nm upon irradiation. The calculations predict two transitions **1** $^2A' \leftarrow$ **X** $^2A'$ and **2** $^2A' \leftarrow$ **X** $^2A'$ at 2.28 and 2.56 eV, with oscillator strength 0.01 and 0.002. The computed energies and the intensities agree well with the matrix spectrum with onsets at 530.3 nm (2.34 eV) and 479.5 nm (2.58 eV). Three absorption bands located 493, 542 and 953 cm^{-1} above the origin of the first electronic system are assigned to the excitation of the ν_{14}, ν_{13} and ν_9 modes (a′) on the basis of their proximity to the MP2 calculated ground state vibrational frequencies 508, 587 and 952 cm^{-1}. Table 1 lists the wavelengths of the absorption band maxima and the assignment for isomer **E•**.

4. Concluding Remarks

The open chain isomers $\mathbf{B}^+$ and $\mathbf{C}^+$ and $\mathbf{A}^+$ with a three membered carbon ring were identified in the neon matrix after trapping of $C_7H_3^+$ produced from indene and acyclic precursors. Cation $\mathbf{B}^+$ exhibits vibrationally structured fluorescence following excitation into the absorption bands of the **1** $^1A_1 \leftarrow$ **X** $^1A_1$ system. No fluorescence was detected for the isomers $\mathbf{A}^+$ and $\mathbf{C}^+$. Weak absorptions of neutral C_7H_3 isomers are also present which gain in intensity upon photobleaching of the cations. Increase in intensity of the absorptions of the neutrals and l-HC_7H^+ is observed after deposition of $C_7H_3^+$ at ~90 eV, a higher kinetic energy. This indicates that fragmentation of $C_7H_3^+$ with ~90 eV deposition energy is mild and only one hydrogen atom is removed. Enhancement of the absorptions of **E•** in higher kinetic energy

experiments suggest that besides the fragmentation, rearrangement of hydrogen atoms takes place upon collisional impact of $C_7H_3^+$ with the neon surface. Isomer $\mathbf{E}^\bullet$ is a secondary product as the $\mathbf{E}^+$ lies 450 kJ/mol above of the lowest energy isomer $\mathbf{A}^+$, and is unlikely to be formed in the source.

Assignment of the absorption systems of the $C_7H_3^+$ and $C_7H_3^\bullet$ isomers is based on CASPT2 calculations of the vertical excitation energies. The assignment is supported by comparison of the calculated harmonic vibrational frequencies with the ones derived from the spectra.

The first observation and identification of the electronic absorptions of the $C_7H_3^+$ and $C_7H_3^\bullet$ isomers in a neon matrix is a starting point for gas phase studies. The knowledge of electronic transitions of the $C_7H_3^+$ and $C_7H_3^\bullet$ isomers provides the means for their in situ monitoring in flames and combustion processes and could lead to a better understanding of polycyclic hydrocarbon formation.

Acknowledgement: This work is supported by the Swiss National Science Foundation (project 200020-124349/1).

References

1. K-H. Homann, *Angew. Chem. Int. Ed.*, 1998, **37**, 2434-2451.

2. C. S. McEnally, L. D. Pfefferle, B. Atakan andK. Kohse-Hoinghaus, *Prog. Energy Combust. Sci.* 2006, **32**, 247-294.

3. K. Kohse-Hoinghaus, B. Atakan, A. Lampprecht, G. G. Alatorre, M. Kamplus, T. Kasper and N-N. Liu, *Phys. Chem. Chem. Phys.* 2002, **4**, 2056-2062.

4. J. Appel, H. Bockhorn, M. Frenklach, *Combust. Flame*.2000, **121**, 122-136.

5. J. Vandooren and V. Detilleux, *J. Phys. Chem. A.* 2009, **113**, 10913-10922.

6. N. Hansen, T. Kasper, S. J. Klippenstein, P.R.Westmoreland, M.E. Law, C.A. Taatjes, K. Kohse-Hoinghaus, J. Wang and T.A. Cool, *J. Phys. Chem. A.* 2007, **111**, 4081-4092.

7. G. Da Silva and W. J. Bozzelli, *J. Phys. Chem. A.* 2009,**113**, 12045-12048.

8. G. da Silva and J. A. Trevitt, *Phys. Chem. Chem. Phys*. 2011, **13**, 8940-8952.

9. G. da Silva, J. A. Trevitt, M. Steinbauer, P. Hemberger, *Chem. Phys. Lett*. 2011, **517**, 144-148.

10. H. Richter and J.B. Howard, *Phys. Chem. Chem. Phys.* 2002, **4**, 2038-2055.

11. J.A. Miller and C. F. Melius, *Combust. Flame.* 1992, **91**, 21-39.

12. J.A. Miller and S. J Klippevstein, *J. Phys. Chem. A*.2003, **107**, 7783-7799.

13. K. Tanaka, Y. Sumiyoshi, Y. Oshima, Y. Endo and K. Kawagauchi, *J. Chem. Phys.*1997, **107**, 2728-2733.

14. K. Tanaka, T. Harada, K. Sakaguchi, K. Harada and T. Tanaka, *J. Chem. Phys.*1995, **103**, 6450-6458.

15. L. Yuan, J. DeSain and R. F. Curl, *J. Mol. Spectrosc.* 1998, **187**, 102-108.

16. T. Gilbert, R. Pfab, I. Fischer and P. Chen, *J. Chem. Phys.* 2000, **112**, 2575-2578.

17. D. A. Ramsay and P. Thistlethwaite, *Can. J. Phys.* 1966, **44**, 1381-1387.

18. A. Fahr, P.Hassanzadeh, B. Laszlo and R. E. Huie, *Chem. Phys*. 1997, **215**, 59-66.

19. M. Wyss, E. Riaplov and J. P. Maier, *J. Chem. Phys.* 2001, **114**, 10355-10361.

20. A. M. Ricks, G. E.Douberly, P. R. Schleyer andM. A.Duncan, *J. Chem. Phys.* 2010, **132**, 051101-051101(4).

21 A. M. Mebel, S. H. Lin, X. M. Yang and Y. T Lee,. *J. Phys. Chem. A.* 1997, **101**, 6781-6789.

22. D. S. N. Parker, F. Zhang, Y. S. Kim and R. I. Kaiser, *J. Phys. Chem. A.* 2011, **115**, 593-601.

23. H. Ding, T. Pino, F. Güthe and J. P. Maier, *J. Am. Chem. Soc.* 2003, **125**, 14626-14630.

24. M. C. McCarthy and P. Thaddeus, *Chem. Soc. Rev.* 2001, **30**, 177-185.

25. T. J. Balle and W. H. Flygare, *Rev. Sci. Instrum*. 1981, **52**, 33-45.

26. M. C. McCarthy, M. J. Travers, A. Kovacs, C. A. Gottlieb and P. Thaddeus, *J. Astrophys. Suppl. Ser.* 1997, **113,** 105-120.

27. V. G. Kunde, A. C. Aikin, R. A. Hanel, D. E. Jennings, W. C. Maguire, R. E. Samuelson, *Nature* 1981, **292**, 686-688.

28. A. Nagy, I. Garkusha, J. Fulara and J. P. Maier, *Phys. Chem. Chem. Phys*. 2013, **15**, 19091-19101.

29. R. Rossetti and L. E. Brus, *Rev. Sci. Inst.* 1980, **51**, 467-470.

30. J. Fulara, A. Nagy, I. Garkusha and J. P. Maier, *J. Chem. Phys*. 2010, **133,** 024304-024304(9).

31. J. Fulara, P. Freivogel, D.Forney and J. P. Maier, *J. Chem. Phys*. 1995, **103**, 8805-8810.

32. M. J. Frisch, G. W. Trucks, H. B. Schlegel, G. E. Scuseria, M. A. Robb, J. R. Cheeseman, J. A. Montgomery, Jr., T. Vreven, K. N. Kudin, J. C. Burant, J. M. Millam, S. S. Iyengar, J. Tomasi, V. Barone, B. Mennucci, M. Cossi, G. Scalmani, N. Rega, G. A. Petersson, H. Nakatsuji, M. Hada, M. Ehara, K. Toyota, R. Fukuda, J. Hasegawa, M. Ishida, T. Nakajima, Y. Honda, O. Kitao, H. Nakai, M. Klene, X. Li, J. E. Knox, H. P. Hratchian, J. B. Cross, V. Bakken, C. Adamo, J. Jaramillo, R. Gomperts, R. E. Stratmann, O. Yazyev, A. J. Austin, R. Cammi, C. Pomelli, J. W. Ochterski, P. Y. Ayala, K. Morokuma, G. A. Voth, P. Salvador, J. J. Dannenberg, V. G. Zakrzewski, S. Dapprich, A. D. Daniels, M. C. Strain, O. Farkas, D. K. Malick, A. D. Rabuck, K. Raghavachari, J. B. Foresman, J. V. Ortiz, Q. Cui, A. G. Baboul, S. Clifford, J. Cioslowski, B. B. Stefanov, G. Liu, A. Liashenko, P. Piskorz, I. Komaromi, R. L. Martin, D. J. Fox, T. Keith, M. A. Al-Laham, C. Y. Peng, A. Nanayakkara, M. Challacombe, P. M. W. Gill, B. Johnson, W. Chen, M. W. Wong, C. Gonzalez, and J. A. Pople, *Gaussian 03, Revision C.02, Gaussian, Inc., Wallingford CT*, 2004.

33. C. Møller, M. S. Plesset, Phys. Rev. 1934, **46**, 618-622.

34. K. Andesson, P.-A. Malmqvist, B. O. Roos, A. J. Sadlej and K. Wolinski, *J. Phys. Chem.* 1990, **94**, 5483-5488.

35. K. Andesson, P.-A. Malmqvist and B. O. Roos, *J. Chem. Phys.* 1992, **96**, 1218-1226.

36. J. Fulara, M. Grutter and J. P. Maier, *J. Phys. Chem. A*. 2007, **111**,11831-11836.

37. A. Batalov, J. Fulara, I. Snitko and J. P. Maier, *J. Phys. Chem. A*. 2006, **110**, 10404-10408.

Figures:

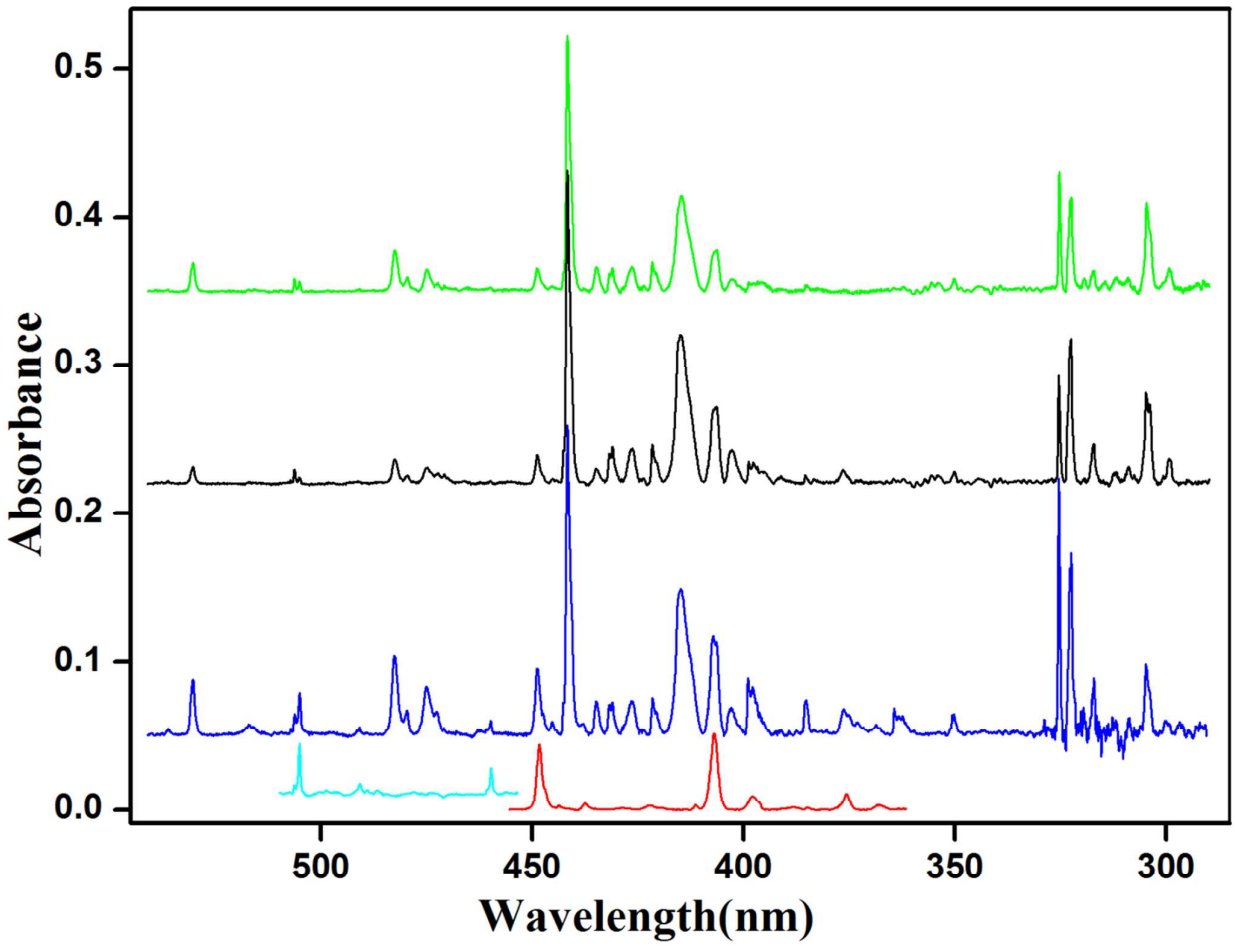

Figure 1. Overview of the absorption spectra of $C_7H_3^+$ recorded in neon matrices: after deposition of $C_7H_3^+$ (black), after 30 min irradiation by a medium pressure mercury lamp λ >260 nm (green) and after deposition of high kinetic energy (~90 eV) cations (blue). The transitions of *l*-HC_7H^+ (red) and *l*-$HC_7H^{\bullet}$ (light blue) were identified in the earlier studies.[30,31]

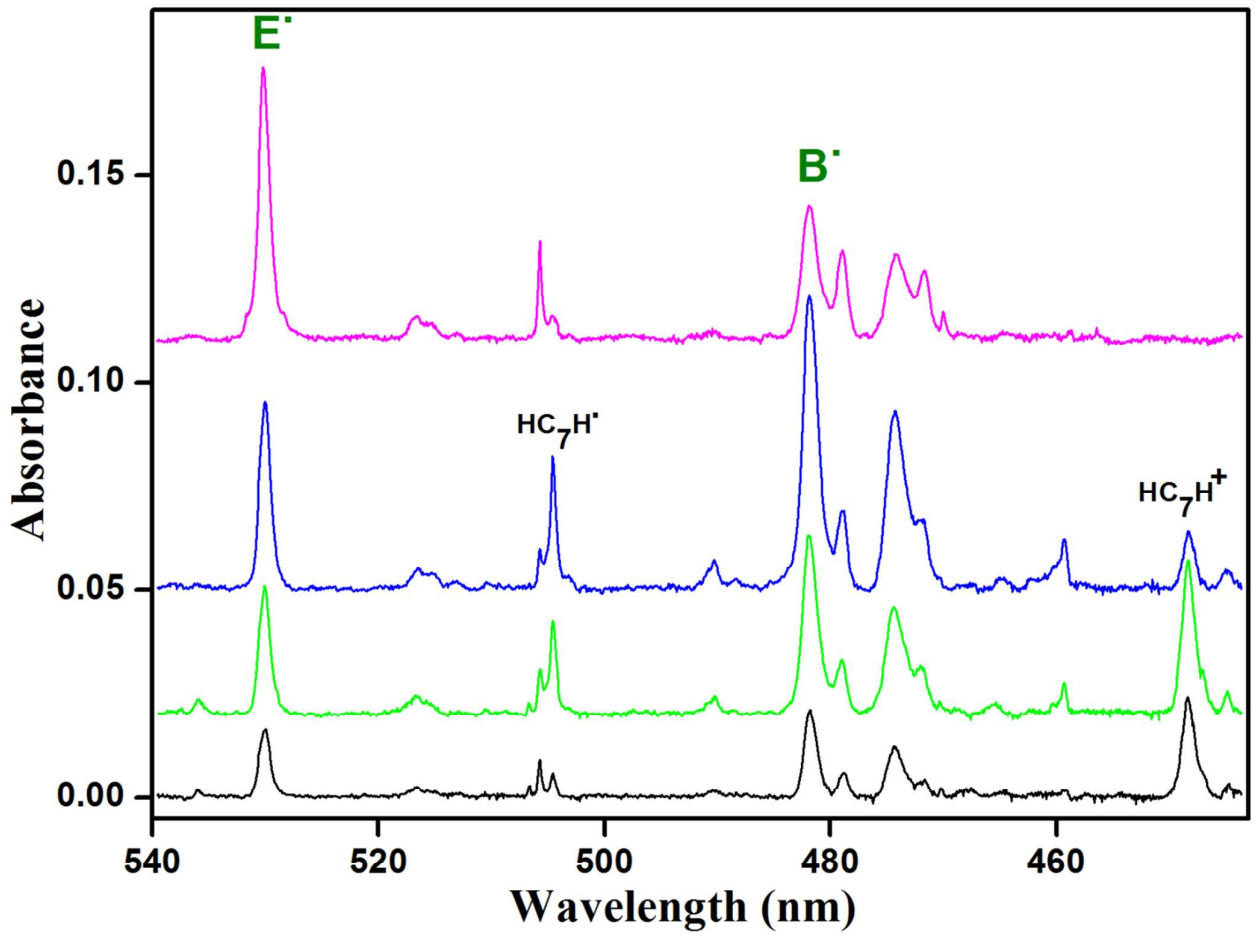

Figure 2. Section of the absorption spectra recorded: after deposition of $C_7H_3^+$ with ~50 eV deposition energy (black), after 30 min irradiation by a medium pressure mercury lamp λ >260 nm (green), after deposition of $C_7H_3^+$ cations with kinetic energy ~90 eV (blue) and after depositing $C_7H_3^-$ followed by irradiation (pink).

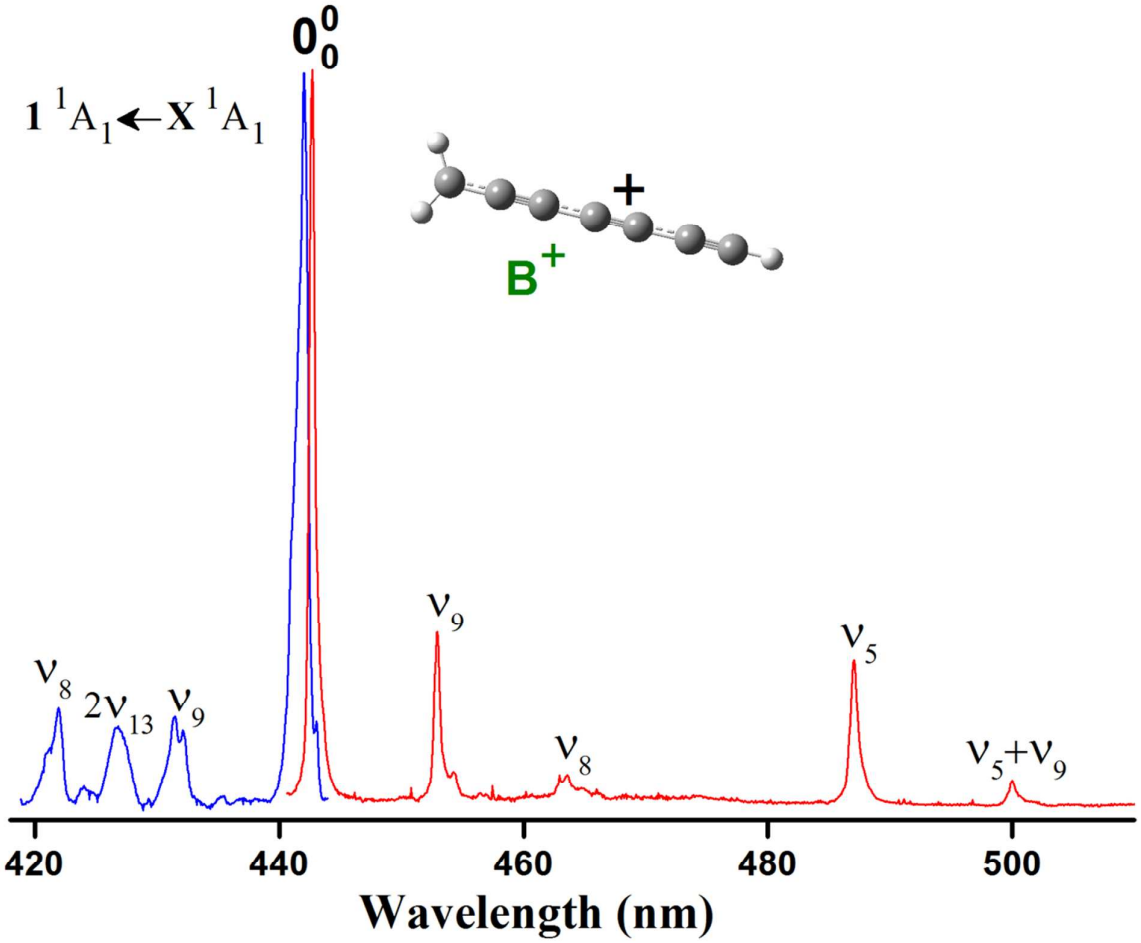

Figure 3. Electronic absorption (blue trace) and fluorescence (red trace) spectra of isomer $\mathbf{B}^+$ recorded in a neon matrix at 6 K. The fluorescence was recoded after exciting the ν_9 absorption band of the $\mathbf{1}\ ^1A_1 \leftarrow \mathbf{X}\ ^1A_1$ transition. The assignments are made on the basis of calculated totally symmetric ground state frequencies.

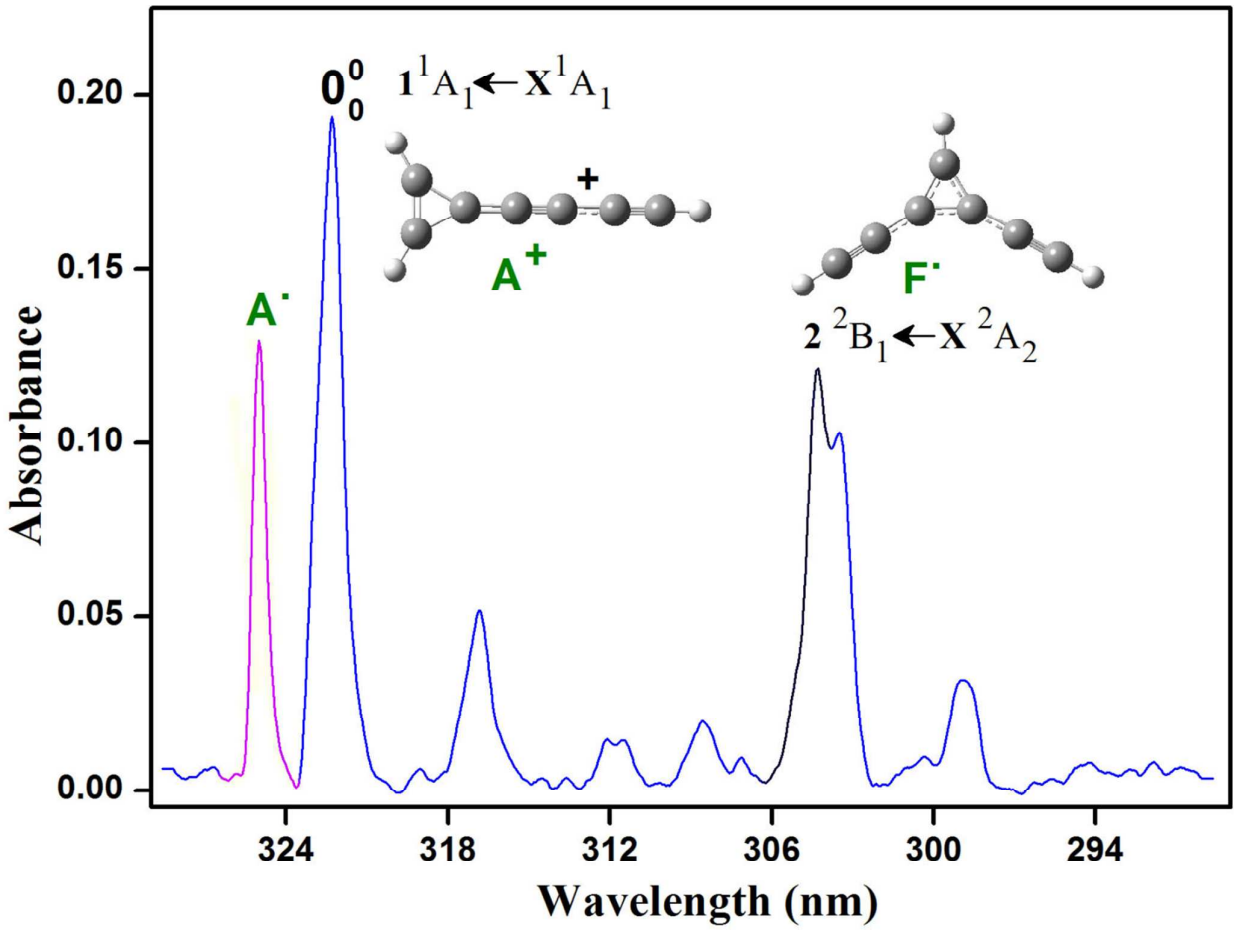

Figure 4. The UV part of the absorption spectrum of $C_7H_3^+$ recorded in a neon matrix followed a mass selective deposition of *m/z* = 87 cations. The absorptions of $\mathbf{A}^+$ (blue), $\mathbf{A}^\bullet$ (pink) and $\mathbf{F}^\bullet$ (black) are indicated.

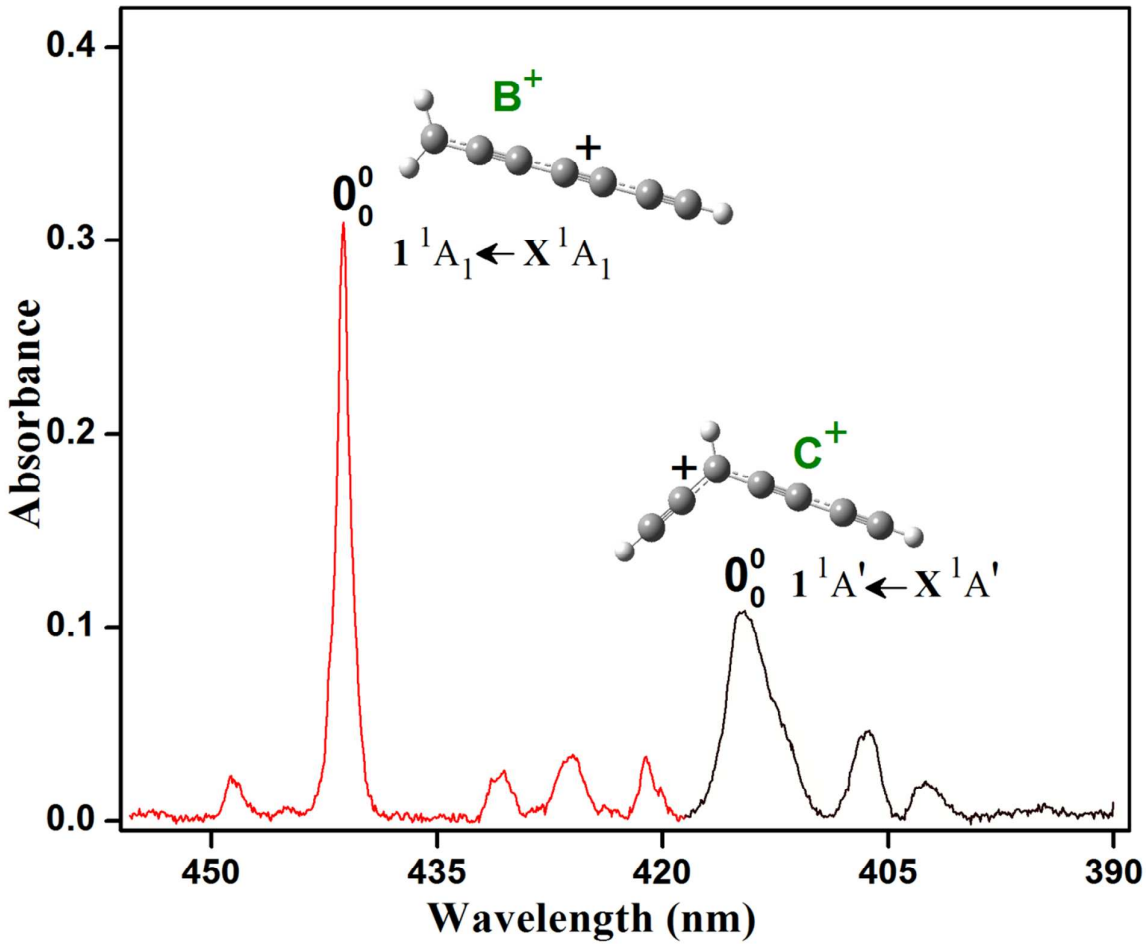

Figure 5. Visible portion of the absorption spectrum showing two electronic systems of the $\mathbf{B}^+$ (red) and $\mathbf{C}^+$ (black) isomers of $C_7H_3^+$ obtained after mass selected deposition of m/z = 87 cations in a neon matrix.

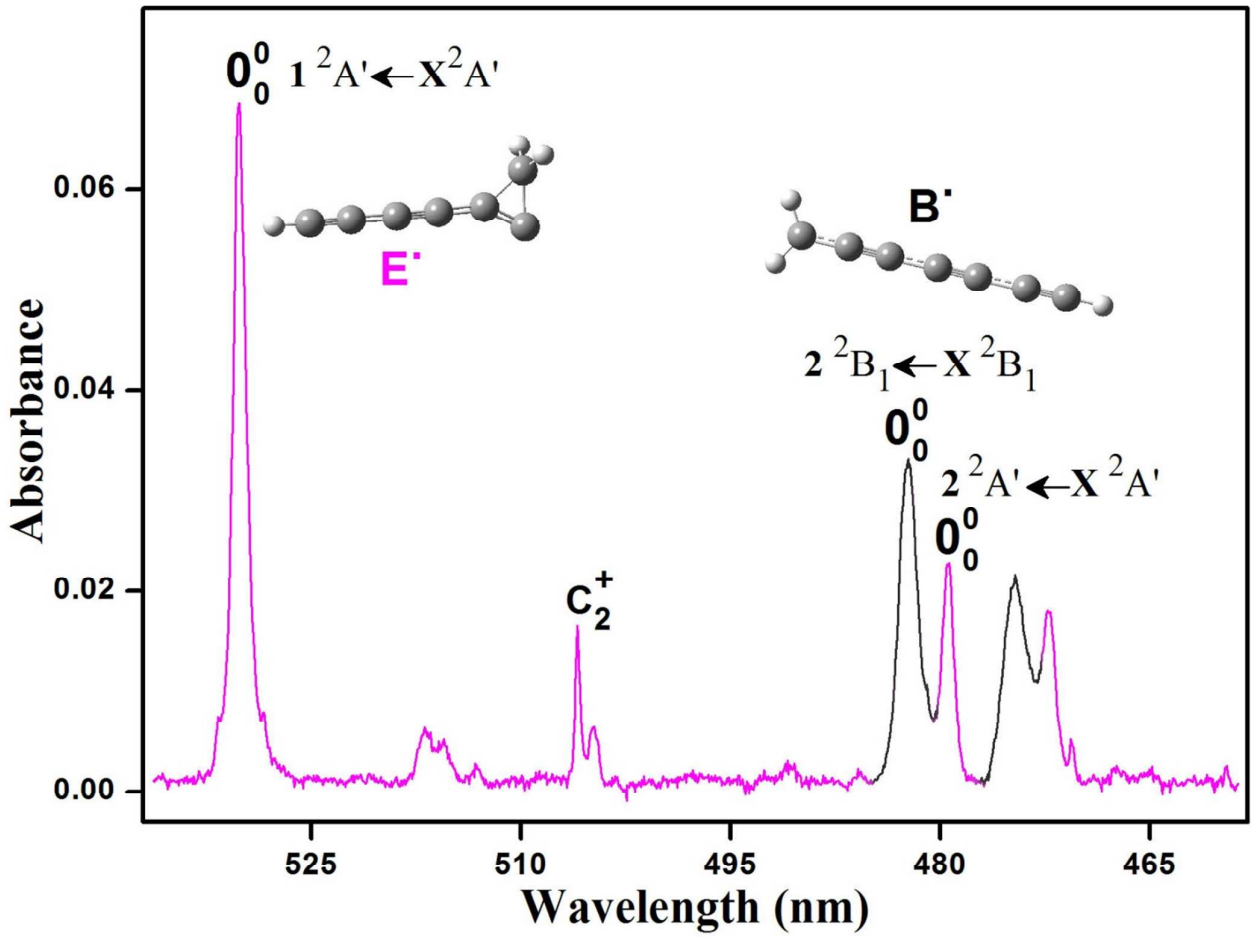

Figure 6. Visible section of the absorption spectrum showing the electronic systems of the **B**$^{\bullet}$ (black) and **E**$^{\bullet}$ (pink) isomers of $C_7H_3^{\bullet}$. The spectrum was measured after a mass – selective deposition of $C_7H_3^-$ (m/z = 87) anion.

Chart1. Structure and relative ground state energy (kJ mol^{-1}) of the five isomers of $C_7H_3^+$ and $C_7H_3^{\bullet}$ calculated with DFT (**bold**) and MP2 level of theory (*italic*) using cc-pVDZ basis set. The corresponding $C_7H_3^-$ anions have been optimized in DFT using aug-cc-pVDZ basis set. Bond lengths (Å) given correspond to the cations optimized with the MP2 method.

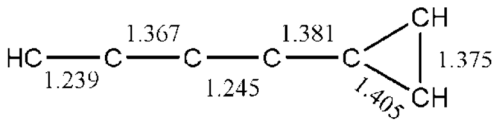

A$^+$ (0,*0*)
A$^{\bullet}$ (86, *160*)
A$^-$ (210)

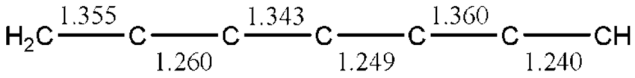

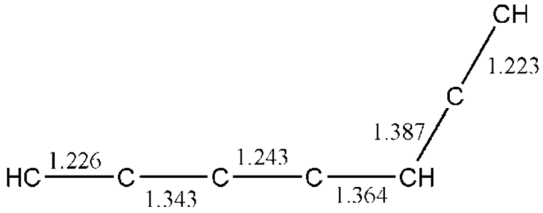

476

B$^+$ (15,*61*)
B$^{\bullet}$ (0,*52*)
B$^-$ (35)

C$^+$ (46,*69*)
C$^{\bullet}$ (28,*29*)
C$^-$ (0)

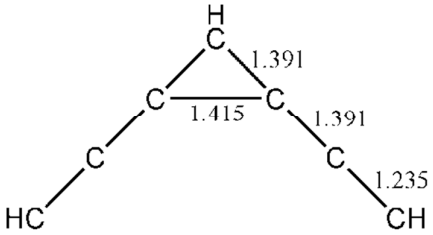

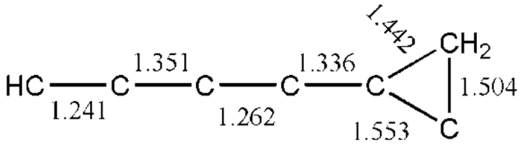

F$^+$ (14, *25*)
F$^{\bullet}$ (104,*134*)
F$^-$ (235)

E$^+$ (381,*452*)
E$^{\bullet}$ (34 ,*281*)
E$^-$ (124)

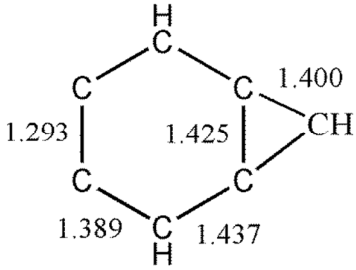

J$^+$ (73,*40*)
J$^{\bullet}$ (- ,*0*)

Table 1. Absorption band maxima (±0.1 nm) in the electronic transitions of $C_7H_3^+$ and $C_7H_3^{\bullet}$ isomers in neon matrices at 6 K. The assignment is based on the calculated harmonic frequencies of the totally symmetric vibrations given in the footnote and Table S3.

	λ (nm)	ν (cm^{-1})	Δν (cm^{-1})	Assignment	
	A^+				
	322.2	31037	0	0_0^0	**1** $^1A_1 \leftarrow$ **X** $^1A_1$
	316.8	31566	529	ν_9	
	303.2	32982	1945	ν_4	
	298.5	33501	2464	$\nu_9+\nu_4$	
	B^+				
	441.3	22660	0	0_0^0	**1** $^1A_1 \leftarrow$ **X** $^1A_1$
	430.9	23218	558	ν_9	
	426.1	23469	809	$2\nu_{21}$	
	421.2	23747	1087	ν_8	
	$B^{\bullet}$				
	482.3	20734	0	0_0^0	**1** $^2B_1 \leftarrow$ **X** $^2B_1$
	474.6	21070	337	$2\nu_{15}$	
	C^+				
	414.6	24120	0	0_0^0	**1** $^1A' \leftarrow$ **X** $^1A'$
	406.6	24592	462	ν_{14}	
	402.5	24845	725	ν_{10}	
	$E^{\bullet}$				
	530.3	18857	0	0_0^0	**1** $^2A' \leftarrow$ **X** $^2A'$
	516.8	19350	493	ν_{14}	

515.5	19399	542	ν_{13}		
504.8	19810	953	ν_9		
479.4	20859	0	0_0^0	**2** $^2A' \leftarrow$ **X** $^2A'$	
472.2	21177	318	ν_{15}		

Totally-symmetric vibrations (all in cm^{-1}) of the identified species calculated at the MP2 /cc-pVDZ level:

A^+ (a_1)**:** $\nu_1 - \nu_9$: 3451, 3314, 2378, 2098, 1739, 1425, 1114, 929, 538;

B^+ (a_1)**:** $\nu_1 - \nu_9$: 3442, 3157, 2543, 2245, 2088, 1532, 1431, 1049, 545;

$B^\bullet$ (a_1)**:** $\nu_1 - \nu_9$: 3669, 3239, 3021, 2711, 2247, 1472, 1083, 1008, 537;

C^+ (a')**:** $\nu_1 - \nu_{17}$: 3440, 3435, 3164, 2495, 2199, 2115, 1471, 1260, 1068, 776, 710, 685, 507, 472, 267, 179, 65;

$E^\bullet$ (a')**:** $\nu_1 - \nu_{16}$: 3647, 3045, 2955, 2553, 1621, 1353, 1217, 1098, 952, 947, 801, 744, 587, 508, 269, 109.

Table 2. Fluorescence band maxima (±0.1 nm) of the **1** $^1A_1 \rightarrow$ **X**$^1A_1$ electronic transition of isomer $\mathbf{B}^+$ trapped in a neon matrix at 6 K. The assignment is based on the calculated harmonic vibrational frequencies given in the footnote of Table 1.

λ (nm)	ν (cm^{-1})	Δν (cm^{-1})	Assignment	
442.7	22589	0	0_0^0	**1** $^1A_1 \rightarrow$**X**$^1A_1$
452.9	22080	509	ν_9	
463.6	21570	1019	ν_8	
487.0	20534	2055	ν_5	
500.0	20000	2589	$\nu_9+\nu_5$	
513.5	19474	3115	ν_2	

Table 3. Electronic excitation energies E_{cal} (eV) and oscillator strength (f) of the dipole allowed electronic transitions for $C_7H_3^+$ and C_7H_3 isomers calculated by the MS CASPT2 method and comparison to the experiment E_{exp}.

	Transitions	E_{cal}	f	E_{exp}
$\mathbf{A}^+$	$\mathbf{X}^1A_1 \rightarrow \mathbf{1}^1A_1$	**4.13**	0.40	3.85
	$\rightarrow \mathbf{2}^1A_1$	5.99	0.0050	
$\mathbf{A}^\bullet$	$\mathbf{X}^2B_1 \rightarrow \mathbf{1}^2A_2$	1.72	0.0020	
	$\rightarrow \mathbf{3}^2B_1$	4.76	0.13	3.82
$\mathbf{B}^+$	$\mathbf{X}^1A_1 \rightarrow \mathbf{1}^1A_1$	**2.99**	0.33	2.81
	$\rightarrow \mathbf{2}^1A_1$	3.95	0.016	
	$\rightarrow \mathbf{3}^1A_1$	4.21	0.0030	
	$\rightarrow \mathbf{4}^1A_1$	5.53	0.0050	
$\mathbf{B}^\bullet$	$\mathbf{X}^2B_1 \rightarrow \mathbf{1}^2B_1$	**2.46**	0.0020	2.57
	$\rightarrow \mathbf{2}^2B_1$	5.73	0.0007	
$\mathbf{C}^+$	$\mathbf{X}^1A' \rightarrow \mathbf{1}^1A'$	**3.13**	0.64	2.99
	$\rightarrow \mathbf{2}^1A'$	4.17	0.030	
	$\rightarrow \mathbf{3}^1A'$	4.73	0.0008	
	$\rightarrow \mathbf{4}^1A'$	5.19	0.040	
$\mathbf{C}^\bullet$	$\mathbf{X}^2A'' \rightarrow \mathbf{1}^2A''$	3.21	0.030	not observed (n.o.)
	$\rightarrow \mathbf{2}^2A''$	4.42	0.010	
	$\rightarrow \mathbf{3}^2A''$	5.08	0.0080	
	$\rightarrow \mathbf{4}^2A''$	5.57	0.020	

E$^{\bullet}$	**X** ^{2}A'→**1** ^{2}A'	**2.28**	0.010	2.34
	→**2** ^{2}A'	**2.56**	0.0020	2.58
	→**3** ^{2}A'	3.43	0.0009	
	→**4** ^{2}A'	3.86	0.0050	
	→**5** ^{2}A'	5.30	0.020	
E^{+}	**X** ^{1}A'→**1** ^{1}A'	0.68	0.0002	n.o.
	→**2**^{1}A'	2.94	0.030	
	→**3**^{1}A'	3.1	0.17	
	→**4**^{1}A'	3.26	0.030	
F^{+}	**X**^{1}A$_1$→**1**^{1}A$_1$	5.46	0.13	n.o.
	→**2**^{1}A$_1$	6.15	0.0090	
F$^{\bullet}$	**X**^{2}A$_2$→**1**^{2}B$_1$	1.15	0.031	
	→**2**^{2}B$_1$	**4.44**	0.042	4.1
	→**3**^{2}B$_1$	5.67	0.19	
J^{+}	**X**^{1}A$_1$→**1**^{1}B$_2$	4.30	0.064	n.o.
	→**1**^{1}B$_2$	5.80	0.003	
	→**1**^{1}A$_1$	5.29	0.013	
	→**2**^{1}A$_1$	5.89	0.11	
J$^{\bullet}$	**X**^{2}B$_1$→**1**^{2}B$_1$	3.36	0.055	n.o.
	→**2**^{2}B$_1$	4.84	0.074	
	→**3**^{2}B$_1$	6.42	0.19	
	→**3**^{2}A$_2$	3.30	0.021	
	→**4**^{2}B$_1$	5.25	0.063	

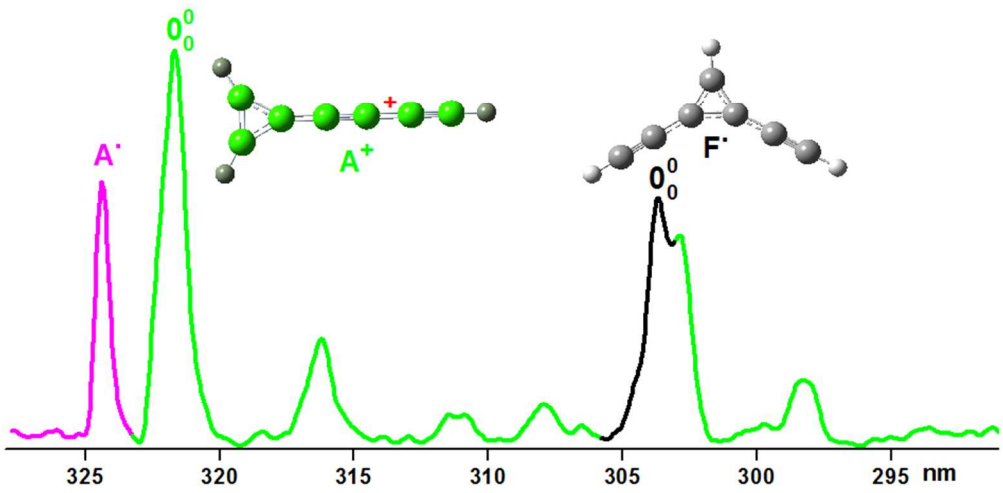

Electronic absorption spectra of mass-selected C7H3+ and C7H3• isomers in a neon matrix have been identified for the first time.
79x39mm (300 x 300 DPI)

Electronic absorption spectra of mass-selected $C_7H_3^+$ and $C_7H_3^\bullet$ isomers in a neon matrix have been identified for the first time.